Solvatochromism and Prototropism in 2-(Aminophenyl)benzothiazoles

Joy Krishna Dey and Sneh K. Dogra*
Department of Chemistry, Indian Institute of Technology, Kanpur 208016, India
(Received February 12, 1991)

The absorption and fluorescence spectra of 2-(2-aminophenyl)-, 2-(3-aminophenyl)-, and 2-(4-aminophenyl)benzothiazoles (*o*-APBT, *m*-APBT, and *p*-APBT, respectively) have been studied in different solvents and at various acid/base concentrations. The ultraviolet and fluorescence spectra and the low pK_a value for the monocation–neutral equilibrium have indicated the presence of an intramolecular hydrogen bond (IHB) in *o*-APBT in the S_0 state. Excited state intra-molecular proton transfer (ESIPT) in *o*-APBT, gives rise to a non-fluorescent phototautomer. Large solvatochromic shifts in polar solvents have indicated the increase in the dipolemoment of *m*-APBT in S_1 state. It has been observed that in protic solvents, *m*-APBT forms a complex with solvent molecule in the S_1 state. The equilibrium constants for different prototropic equilibria of the molecules have been determined in both S_0 and S_1 states. The absorption and fluorescence spectra of the prototropic species have been explained and compared with those of 2-phenylbenzothiazole (2-PBT). The monocation (**2**) of *p*-APBT, formed by protonation at the $-NH_2$ group is found to undergo structural reorganization leading to a quinonoid structure (**2'**). The absorption and fluorescence excitation spectra (recorded at 390 nm and 460 nm fluorescence bands) indicate the simultaneous presence of species (**2**) and (**2'**), the former being more favorable in protic and the latter in nonpolar solvents. The molecular orbital calculation (PPP) has been used to calculate the absorption spectra and the charge densities at the basic centers of the neutral molecules.

The study of photophysical properties of heterocyclic organic molecules has achieved considerable importance recently because many of these molecules form an integral part of biologically important compounds and have various uses. Substituted 2-arylbenzothiazoles, although having industrial and commercial uses as fluorescence whitening agents,[1a] photoconducting materials,[1b] and as herbicides in agriculture, have not received much attention. Only 2-(2-hydroxyphenyl)-benzothiazole[2] has been studied extensively and the excited state intramolecular proton transfer (ESIPT) has been well discussed. The present study is centerd on the prototropism and solvatochromism of *o*-APBT, *m*-APBT and *p*-APBT. Since the amino group is strong electron donor in the excited state, the position of the fluorescence spectrum may exhibit a pronounced solvent dependence, but the absorption spectrum is almost insensitive to the nature of the solvent. The importance of this type of molecules (i.e. aromatic amines) in biological studies has led to intensive investigation of the origin of the polar-solvent-induced fluorescence red shift.

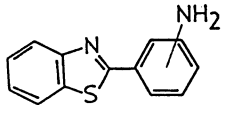

$-NH_2$ at 2'-
3'-
4'-

In our recent studies on (aminophenyl)benzimidazoles[3] and (aminophenyl)benzoxazoles,[4] it has been shown that 2-(2-aminophenyl)benzimidazole[3b] (*o*-APBI) exhibits a dual fluorescence in hydrocarbon solvents, whereas, the corresponding benzoxazole derivative[4] (*o*-APBO) gives only a single normal fluorescence band. The dual fluorescence in the former, has been attributed to a phototautomer formed by ESIPT process. The absorption spectra of the monocations of both *p*-APBI and *p*-APBO showed a large red-shifted band along with the blue-shifted band, the origin of which was unknown until the present study. The monocations of *o*-APBO, *m*-APBO, and *p*-APBO were found to undergo biprotonic phototautomerism in the S_1 state.

In order to understand these processes we have undertaken this investigation to include a detailed analysis of the electronic absorption and emission spectra of *o*-APBT, *m*-APBT, and *p*-APBT including 2-PBT and their prototropic species. In addition we have carried out molecular orbital calculation (PPP-SCF-MO-CI) to aid the interpretation of our experimental results.

Experimental

The compounds under study were synthesised by heating *o*-aminothiophenol and corresponding aminobenzoic acid in polyphosphoric acid at 200 °C and purified as described for (aminophenyl)benzoxazole.[5] The purity of the compounds was confirmed by TLC, melting point and excitation spectra recorded in methanol monitoring at different emission wavelengths. Analytical grade cyclohexane (SDS), dioxane (E. Merck), acetonitrile (E. Merck), methanol (BDH), and dichloromethane (E. Merck) were further purified as described elsewhere.[6] Analytical grade ethanediol (SDS) and glycerol (SDS) were used directly. Hexane (SRL), ethyl acetate (SDS), chloroform (SDS), and carbon tetrachloride (SDS) were all spectro grade. KOH, H_2SO_4, and ortho-H_3PO_4 used, were of analytical grade.

Aqueous pH solutions were made by mixing appropriate amounts of dilute (10^{-3} M, M=mol dm^{-3}) KOH and H_3PO_4 solutions. Solutions of pH<3 and pH>12 were made following Hammett's[7a] acidity (H_o) and Yagils[7b] basicity scales (H_-). Because of low aqueous solubility of the compounds, the solutions were prepared in methanol–water mixture containing 0.5% (v/v) methanol and the concentration of the solute was 5×10^{-6} M. Fluorescence quantum yields were calculated

for solutions having absorbance <0.1 at the excitation wavelength, and referred to the quinine sulfate in 0.05 M H_2SO_4 (ϕ_f=0.55).[7c] For fluorimetric titrations the solutions were excited at the isosbestic point.

Absorption spectra were measured in a Shimadzu UV-190U spectrophotometer equipped with a 135U chart recorder. Fluorescence spectra were recorded in a scanning spectrofluorimeter fabricated in our laboratory and the details of which are described elsewhere.[8] The pH measurements have been carried out with a Toshniwal Digital pH meter, model CL 46 fitted with a combined glass electrode (Toshniwal) operating in the range of pH 0 to 12.

Molecular orbital calculations were performed on our Institute's Dec-1090 computer. The program[9] for the calculations was obtained from QCPE, Indiana University, Blumington, USA.

Results and Discussion

1. Effect of Solvent on Absorption and Fluorescence Spectra. In Table 1, the absorption properties of the molecules in several organic solvents are indicated. Apart from the shoulder to the lower energy side of the longest wavelength band (ca. 293 nm), the absorption spectrum of *m*-APBT resembles that of 2-phenylbenzothiazole (PBT).[10] The lowest energy band of *p*-ABPT appears at a wavelength higher than that of *m*-APBT. The absorption spectrum of *o*-APBT is quite different from those of other molecules in the sense that apart from the common band (ca. 290 nm) another large red shifted band appears at 365 nm, which disappeared when the solution was made acidic (pH<3.0). These features are exactly analogous to that of *o*-APBI[3b] and *o*-APBO.[4] The second lowest energy absorption band of *o*-APBT is structured in hydrocarbon solvents and becomes broad in polar protic solvents. With the increase of solvent polarity the absorption maxima of the molecules remain almost unchanged except in *o*-APBT where the longest wavelength band shifts to the blue in protic solvents.

Fluorescence spectral data are collected in Table 2. The fluorescence spectra of *m*-APBT and *o*-APBT are broad and structureless, whereas that of *p*-APBT in hydrocarbon solvents is structured. The fluorescence spectra, unlike absorption spectra in all the cases shift to red as the solvent polarity and proton donor/acceptor capacity increased in going from cyclohexane to water. The order of emission energies, *o*-APBT<*m*-APBT<*p*-

Table 1. Absorption Band Maxima (λ_a) and Molar Extinction Coefficients ($\log\varepsilon$) of *o*-APBT, *m*-APBT, and *p*-APBT in Different Solvents and of Different Prototropic Species

Solvent	*o*-APBT		*m*-APBT		*p*-APBT		Solvent	*o*-APBT		*m*-APBT		*p*-APBT	
Species	λ_a	($\log\varepsilon$)	λ_a	($\log\varepsilon$)	λ_a	($\log\varepsilon$)	Species	λ_a	($\log\varepsilon$)	λ_a	($\log\varepsilon$)	λ_a	($\log\varepsilon$)
1	2		3		4		1	2		3		4	
Hexane	375	sh	328	sh	338	sh	1,2-Ethanediol	369		335		335	
	362	(4.12)	293		327					299			
	315	(3.68)			310		Glycerol	367		337		335	
	303	(3.89)								300			
	289	(4.10)					Water (pH 6.3)	351	(4.05)	325	sh	333	(4.41)
	280	(4.03)						289	(4.06)	297	(4.26)		
Cyclohexane	375	sh	328	sh	338	sh							
	363	(4.12)	294		329		Carbon tetra-	375	sh	328	sh	332	(4.49)
	315	(3.52)			310		chloride	365	(4.15)	297	(4.18)		
	304	(4.04)						300	sh				
	290	(4.12)						291	(4.16)				
	280	(4.05)						281	(4.15)				
Acetonitrile	367	(4.11)	330	sh	336	(4.54)	Dichloro-	366	(4.31)	330	sh	332	(4.56)
	315	sh	295	(4.27)			methane	300	sh	295	(4.22)		
	304	sh						291	(4.32)				
	289	(4.11)						280	sh				
	280	sh					Chloroform	366	(4.11)	329	sh	332	(4.49)
Dioxane	370	(4.16)	334	sh	337	(4.54)		300	sh	297	(4.17)		
	300	sh	296	(4.27)				291	(4.11)				
	291	(4.16)						280	sh				
	282	sh					Monocation	303[a]	(4.32)	300[b]	(4.28)	392[c]	(3.86)
Ethyl acetate	372	(4.07)	333	sh	337	(4.5)		250	—	250	—	300	(4.22)
	300	sh	295	(4.27)								251	—
	290	(4.07)					Dication	310	(4.22)	320	(4.33)	320	(4.37)
	281	sh					(H_o −4.0)	252	—	256	—	257	—
Methanol	367	(4.09)	336	sh	334	(4.56)							
	315	sh	294	(4.24)									
	289	(4.14)											

a) at pH 0.5. b) at pH 2.0. c) at pH 1.5.

Table 2. Fluorescence Band Maxima, λ_f(nm) and Fluorescence Quantum Yields (ϕ_f) of *o*-APBT, *m*-APBT, and *p*-APBT in Different Solvents and of Different Prototropic Species

Solvent	*o*-APBT		*m*-APBT		*p*-APBT	
Species	λ_f	ϕ_f	λ_f	ϕ_f	λ_f	ϕ_f
Hexane	—	—	380	0.28	385(sh) 375 360(sh)	0.33
Cyclohexane	410	<0.001	380	0.29	385(sh) 375 360(sh)	0.36
Acetonitrile	435	0.074	440	0.20	400	1.0
Dioxane	425	0.07	420	0.20	395	1.0
Ethyl acetate	435	0.067	430	0.18	400	
Methanol	440	0.132	475	0.14	410	1.0
1,2-Ethanediol	443		490		415	
Glycerol	435		490		418	
Water (pH 6.2)	450	0.22	503	0.06	420	0.97
Carbon tetrachloride	420	0.001	390		385	
Dichloromethane	425	0.011	413	0.141	395	1.0
Chloroform	425	0.011	417	0.13	390	0.82
Monocation	390[a]	0.015	390[b]	0.027	443[c]	<0.001
Dication (H_o −4.0)	420		425	0.027	415	0.022

a) at pH 0.5. b) pH 2.0. c) pH 1.5.

to the resonance interaction of the lone pair of the amino nitrogen atom with the π cloud of the parent hydrocarbon. This interaction increases if an electron withdrawing group is attached at the para position. Thus the nature of electron withdrawing group at the para position decides the percentage charge transfer character in the π→π* transition as well as the value of band maximum. The large red shift observed in the longest wavelength absorption band of *p*-APBT, as compared to that in *m*-APBT, can be attributed to the presence of electron withdrawing group at the para position of aniline and thus leading to the resonance structure **II′** as shown below. This is reflected in the high absorption coefficient (ε_{max}, Table 1) of the lowest energy band, large ϕ_f value (ca. 1.0) and the structured fluorescence band in nonpolar solvents. The presence of structure **II′** can be further established from acid-base behavior of this molecule (see below).

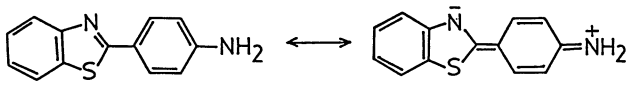

II II′

Scheme 1.

APBT, in cyclohexane changes to the order, *m*-APBT<*o*-APBT<*p*-APBT in polar/protic solvents. The luminescence of *o*-APBT in all the solvents as well as in cyclohexane glass at 77 K exhibits a single fluorescence band at ca. 400 nm.

The fluorescence quantum yield (ϕ_f) of *p*-APBT is almost unity in all the solvents, whereas those of *o*-APBT and *m*-APBT are very rlow. *o*-APBT is weakly fluorescent (ϕ_f<0.001) in hydrocarbon solvents and the ϕ_f increases as the solvent polarity is increased. The ϕ_f value decreases for *m*-APBT with the increase of polarity.

Spectral studies of 2-arylbenzoxazoles and corresponding benzothiazoles by Passarini[10] have indicated that the aryl group acts as the main chromophore and its electronic transitions are perturbed by the benzazole moiety. Our experimental studies as well as molecular orbital (MO) calculations (CNDO/s and PPP) on 2-phenylbenzoxazole[11] have confirmed earlier results and have shown that both HOMO and LUMO are localized mostly on the phenyl ring and only partly on the oxazole ring. This means that the longest wavelength transition originates from the phenyl ring. Since benzoxazole and benzothiazole are isoelectronic, their electronic spectra are expected to be similar. Thus, the (aminophenyl)benzothiazoles can be considered as substituted anilines.

The electronic spectra of arylamines have been studied extensively[12–14] and the red shift produced in the absorption spectra of the parent hydrocarbon is due

Even though the amino group in *m*-APBT is nonconjugated with the electron withdrawing benzothiazole group, the fluorescence spectrum, in contrast to absorption spectrum, is large red shifted. This may be due to larger dipole moment of the fluorophore in the S_1 state upon excitation (section 2). The red shift observed in the fluorescence spectrum in protic polar solvents is anomalously large and could be attributed to the formation of 1 : 1 solvent–solute complex in S_1 state. This is based on the fact that (i) the Stokes shift observed in just 0.5% (v/v) methanol–cyclohexane mixture (where the properties of the solution will be close to cyclohexane) is 6210 cm^{-1} as compared to 8500 cm^{-1} in 100% methanol and (ii) full width at half maximum height of fluorescence band in cyclohexane (2959 cm^{-1}) is quite different from that in 0.5% methanol–cyclohexane solution (5640 cm^{-1}). The similar behavior has been observed in 5-aminoindazole[16a] and other aromatic amines.[16,17] This solute–solvent interaction enhances the stability of the singlet and thereby decreasing the S_1–T_1 energy gap, which in turn increases the probability of intersystem crossing.[18] This fact explains the decrease of ϕ_f value in *m*-APBT with the increase of solvent polarity in going from cyclohexane to water.

The geometry of the molecule suggests the formation of an intramolecular hydrogen bond (IHB) between the pyridinic nitrogen atom and one of the amino protons (conformer IA) in *o*-APBT. We feel that the longest wavelength band is due to the hydrogen-bonded structure IA. This is because the presence of IHB in *o*-

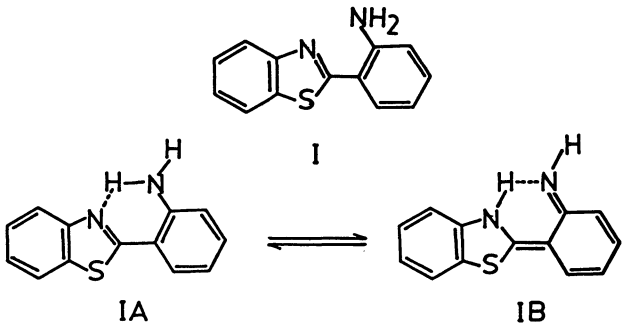

Scheme 2.

APBT will force the lone pair of the amino group to be parallel with the π-cloud and thereby increases the resonance character of this group with the benzothiazole moiety. The blue shift observed in protic solvents can be attributed to the partial breaking of the IHB as a result of competition with the intermolecular hydrogen bond formation with the solvent molecules. Similar behavior has also been observed in case of *o*-APBI[3b] and *o*-APBO[4] and can be explained on the same lines.

It is well known that the amino proton becomes strong acid and the tertiary nitrogen atom strong base in S_1 state. Along with the presence of IHB, this will facilitate the proton transfer giving rise to the phototautomer, IB. Since the rate of ESIPT is very high[2] (ca. 10^{12} s^{-1}) and the activation energy is very low (ca. 120 cm^{-1}), an emission band corresponding to the phototautomer can be expected especially in nonpolar solvents. In contrast, only a weak normal Stokes shifted broad band at 400 nm has been observed in hydrocarbon solvents, as in *o*-APBO.[4] But in case of *o*-APBI,[3b] a dual fluorescence was observed in cyclohexane. This indicates that the phototautomer IB is formed but it is nonfluorescent. It is reported[15] that the ESIPT increases the rate of internal conversion 100 times. The very low ϕ_f (<0.001) of normal Stokes shifted fluorescence band in hydrocarbon solvents proves the conversion of IA→IB. Because of the formation of a solvated complex and breaking of IHB (a prime condition for ESIPT) in polar and protic solvents, the rate of ESIPT is reduced. As a result, ϕ_f of *o*-APBT increases as the solvent polarity increases.

2. Correlation of Solvatochromic Shift with the Solvent Polarity. The variation of Stokes shift with the solvent polarity can be represented by the Lippert[19] equation

$$\bar{\nu}_{ss}=\frac{2(\mu_e-\mu_g)^2}{hca^3}f(D,n)+C, \quad (1)$$

where $\bar{\nu}_{ss}$ is the Stokes shift ($\bar{\nu}_{ss}=\bar{\nu}_a-\bar{\nu}_f$, $\bar{\nu}_a$ and $\bar{\nu}_f$ are the absorption and fluorescence maxima, respectively), μ_g and μ_e are respectively the ground and excited state dipole moments of the solute molecule, '*a*' is the "Onsager cavity radius" and $f(D,n)$ is the "Onsager polarity function" defined by the equation

$$f(D,n)=\frac{D-1}{2D+1}-\frac{n^2-1}{2n^2+1}, \quad (2)$$

where D is the static dielectric constant and n is the refractive index of the solvent; C is a constant. The other polarity parameter used is an empirical parameter $E_T(30)$; this is based on the spectral shifts of *N*-phenolbetaine,[20,21] in different solvents of varying polarity and hydrogen bonding.

In this study, the Stokes shifts of the three molecules determined in eleven solvents of varying polarity have been correlated with the $f(D,n)$[22] and $E_T(30)$[23] parameters. Table 3 gives a list of solvents, corresponding polarity parameters and the Stokes shifts. The very good linearity found in the plot of $\bar{\nu}_{ss}$ vs. $f(D,n)$, Fig. 1, in aprotic solvents (except dioxane and chloromethanes) indicates that the unspecific interactions are the key factors in shifting the fluorescence maxima to the red, for these molecules. As evident from the slopes of the plots, these interactions are large in case of *m*-APBT and may be attributed to its increase of dipole moment on excitation. Rigid molecules with limited internal degrees of freedom change the structure of the solvent cage by their dipole moment change in the excited state. This process induces a large Stokes shift in polar solvents. This is true in nonviscous solvents, where the

Table 3. Stokes Shifts of *o*-APBT, *m*-APBT, and *p*-APBT in Different Solvents and Polarity Parameters

Number	Solvent	$f(D,n)$[a]	$E_T(30)$[b]	$\bar{\nu}_{ss}/cm^{-1}$		
			kcal mol^{-1}	*o*-APBT	*m*-APBT	*p*-APBT
1	Cyclohexane	−0.001	31.07	3160	4170	3610
2	Hexane	0.002	31.0		4170	3610
3	Dioxane	0.02	36.0	3500	6130	4360
4	Ethyl acetate	0.201	38.09	3900	6690	4630
5	Acetonitrile	0.305	46.0	4260	7580	4760
6	Methanol	0.309	55.5	4520	8710	5550
7	1,2-Ethanediol	0.276	56.3	4530	9440	5850
8	Glycerol	0.264	57.0	4260	9270	5940
9	Water	0.320	63.1	6270	10770	6220
10	Dichloromethane	0.218	41.1	3800	6090	4760
11	Chloroform	0.149	39.1	3800	6410	4480

a) Values taken from Ref. 22. b) Values taken from Ref. 23.

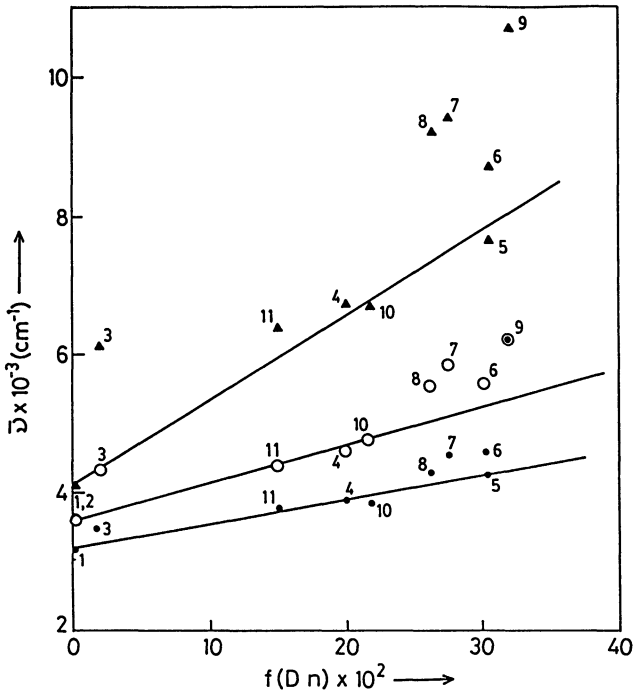

Fig. 1. Plot of $f(D,n)$ parameters revsus $\bar{\nu}_{ss}$ in different solvents: —●— *o*-APBT, —▲— *m*-APBT, and —○— *p*-APBT.

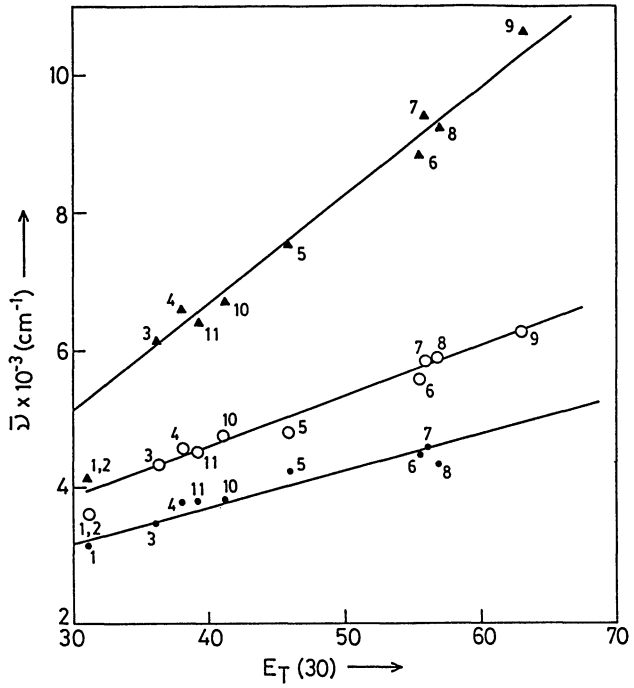

Fig. 2. Plot of $E_T(30)$ parameters versus $\bar{\nu}_{ss}$ in different solvents: —●— *o*-APBT, —▲— *m*-APBT, and —○— *p*-APBT.

rate of solvent relaxation (ca. 10^{12} s^{-1}) is faster than the fluorescence rate (10^9—10^{11} s^{-1}). But in a viscous solvent like glycerol (where the relaxation time is of the order ca. 10^{-9} s) or in a polar solvent at 77 K, the solvent relaxation can not occur during the lifetime of the excited state. The fluorescence spectrum of *m*-APBT in glycerol is broad and has the same shape as in nonviscous solvents and no blue shift is observed compared to other solvents at 300 K. This clearly indicates that the solvent relaxation is still faster than the rate of fluorescence. The anomaly in the solvatochromic shift in dioxane and protic solvents may be a result of hydrogen bond formation between the specific sites of the solute and solvent molecules giving rise to 1 : 1 complex as explained earlier.

A good correlation of Stokes shift with the $E_T(30)$ scale (Fig. 2) is indicative of the fact that the dielectric solute–solvent interactions as well as specific solute–solvent interactions, as discussed above, are responsible for the solvatochromic shifts in the molecules. The Stokes shifts observed for these molecules in chloroform and carbon tetrachloride correlate with none of the polarity scales. It is well known that chlorinated methanes quench the fluorescence of fluorophores by forming a CT in the S_1 state,[24] which may be a reason for the deviation complex of the Stokes shift from linearity of solvatochromic plots in Figs. 1 and 2.

Since the position of fluorescence maximum of *m*-APBT has shown much more solvent dependence than the other molecules, we have also investigated the fluorescence properties of this molecule in dioxane–water mixtures. The dioxane–water mixtures provide a wide range of $E_T(30)$ values and allow a convenient solvent system to probe nonspecific effects on fluorescence maximum. The solvent compositions and the corresponding $E_T(30)$ values alongwith the fluorescence maxima are listed in Table 4. A plot of $\bar{\nu}_f$ versus $E_T(30)$ values (Fig. 3) shows very good correlation. This type of effect has been reported earlier and is attributed to the increasing solvation of the solute molecules in its S_1 state by water molecules which impart an enhanced solvent structuring effect.

Table 4. Fluorescence ($\bar{\nu}_f$) Maxima of *m*-APBT in Different Dioxane–Water Mixture and Corresponding $E_T(30)$ Values

Composition number	% (v/v) Dioxane	$E_T(30)$[a] / $\times 10^3$ cm^{-1}	$\bar{\nu}_f$/cm^{-1}
1	100	12.59	23809
2	98	14.48	22471
3	94	15.56	22222
4	92.5	15.95	21978
5	90	16.33	21505
6	80	17.14	21276
7	70	17.80	21052
8	60	18.29	20920
9	50	18.74	20618
10	40	19.44	20408
11	30	20.00	20408
12	20	20.49	20202
13	10	21.30	20000
14	0	22.00	19880

a) Values taken from Ref. 22.

3. Effect of Hydrogen Ion Concentration. The absorption and fluorescence spectra of all the molecules are studied in various acid-base concentrations in the H_o/pH/H_- range of −10.4 to 16.0 at room temperature (300 K). The spectral properties of their different prototropic species are collected in Tables 1 and 2, and the spectra are shown in Figs. 4 and 5. The behavior of these molecules in the above range of acid-base region is similar, except for *p*-APBT in the pH range of 5 to 1. This will be discussed separately.

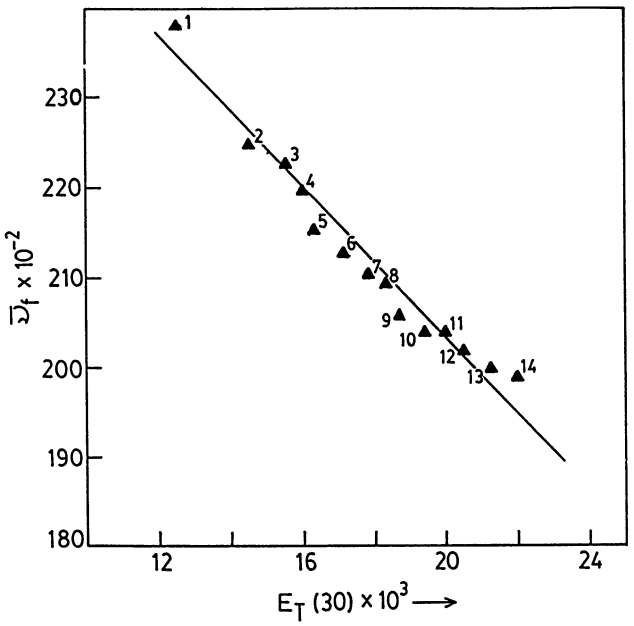

Fig. 3. Plot of $E_T(30)$ parameters versus $\bar{\nu}_f$ in dioxane-water mixtures.

The absorption spectra of *m*-APBT remains unchanged in the pH/H_- range of 5 to 16, but the fluorescence intensity decreases above pH 9. Because of insolubility, neither *o*-APBT nor *p*-APBT could not be studied in the basic media. We attribute the decrease of fluorescence intensity of *m*-APBT with increase of pH to the formation of nonfluorescent monoanion, because the anion formed by the deprotonation of amino group in general is nonfluorescent with few exceptions.[25]

All the molecules are neutral between pH 9 to 5. The blue shift in the absorption and fluorescence spectra and the resemblance of the spectra of these species with those of neutral 2-PBT at pH 4 (λ_a=299 nm, λ_f=380 nm) indicate the formation of monocation as a consequence of the protonation at the amino group. Our theoretical calculations also indicate that the charge density (Table 6) at the amino nitrogen is greater than that at the nitrogen atom of the heterocyclic ring in the S_0 and S_1

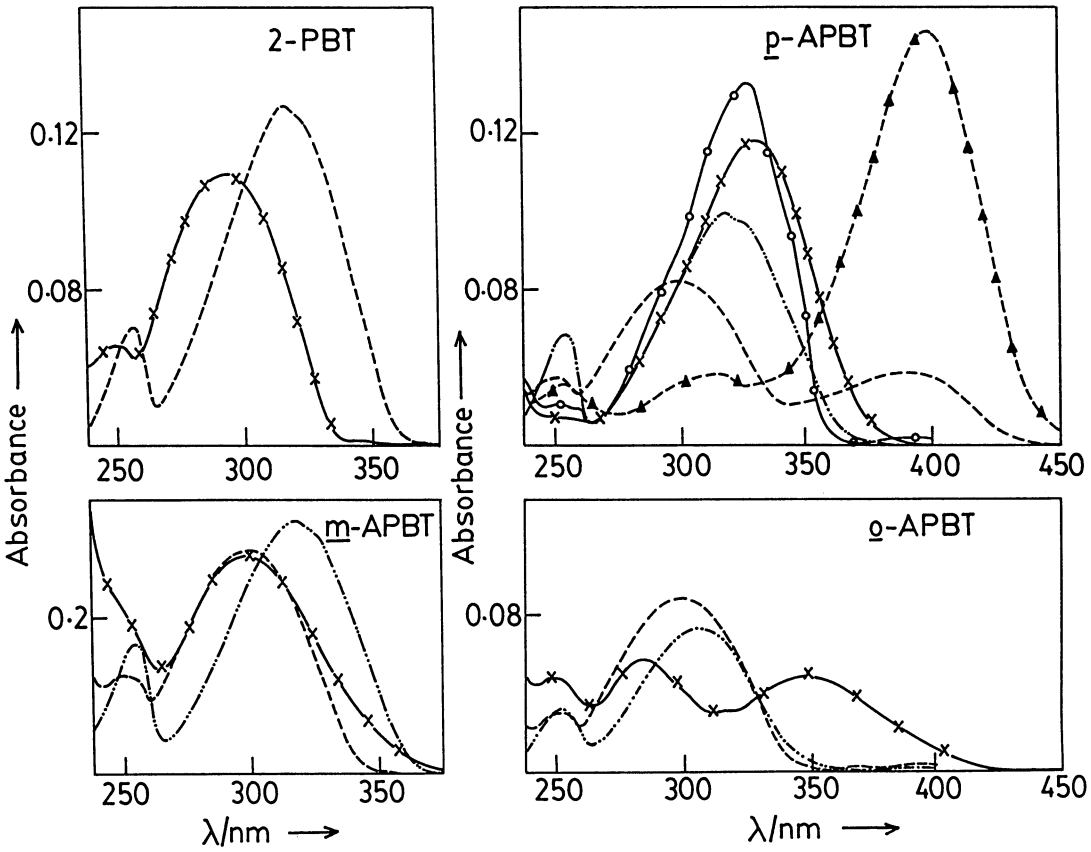

Fig. 4. Absorption spectra of the prototropic species of 2-PBT, *o*-APBT, *m*-APBT, and *p*-APBT; —X— Neutral; —— Monocation; —··— Dication; —▲— Monocation (in cyclohexane); —○— Neutral in cyclohexane.

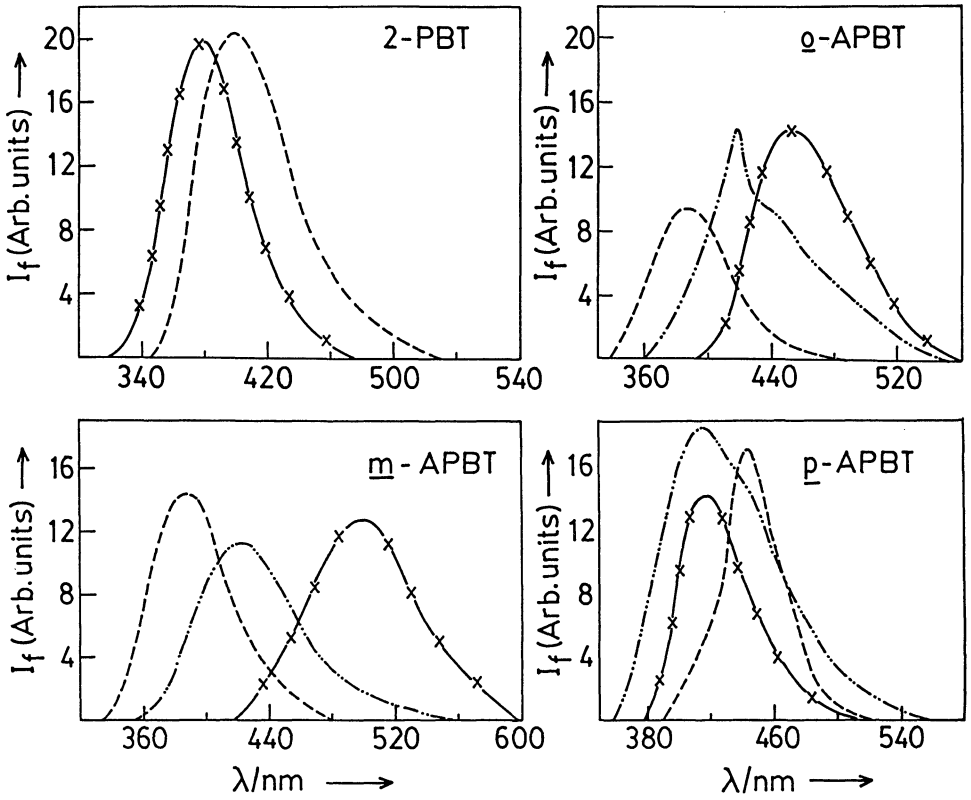

Fig. 5. Fluorescence spectra of the prototropic species of 2-PBT, *o*-APBT, *m*-APBT and *p*-APBT: —×— Neutral; —— Monocation; —··— Dication.

states. The red shift in both the absorption and fluorescence spectra of the monocation below pH 0.5 is due to the dication, formed by the protonation of the pyridinic nitrogen atom and is confirmed by their similarity with the monocation spectra of 2-PBT (λ_a=320 nm, λ_f=400 nm).

The absorption and fluorescence spectral characteristics of *p*-APBT in acidic media are interesting and quite different from those of *o*-APBT and *m*-APBT. With the increase of $[H^+]$ ($>10^{-4}$ M) the intensity of the 333 nm absorption band decreases and at pH 1.5, it is replaced by a large red-shifted band at 392 nm and a blue-shifted band at 300 nm. The intensity of the longest wavelength band is weak compared to the blue-shifted band in aqueous medium. The spectra exhibit two isosbestic points (300 nm and 368 nm). When the titration was carried out in cyclohexane with trifluoroacetic acid, the absorption spectrum of the species (Fig. 4) exhibits the longest wavelength band with much higher intensity compared to the blue shifted band. Further increase of acid concentration shifts the short wavelength band to red side and the lowest energy band is vanished. The absorption spectrum at H_0—4.0 resembles that of the monocation of 2-PBT.

The isosbestic points in the absorption spectra clearly indicate that only two species are involved in the equilibrium. This is also substantiated by the fact that the pK_a values calculated by measuring the intensity change at 390 and 330 nm are exactly same. The pK_a value for this equilibrium (3.0) is not very different from those of *o*-APBT (2.6) and *m*-APBT (3.4). This suggests, and also supported by the charge densities (Table 6) at the basic centers that the species at pH 1.5 is the monocation formed by protonation at the amino group. But, as can be seen from Fig. 4, the monocation spectrum does not resemble the absorption spectrum of 2-PBT. Similar behavior has also been observed in 2-, and 4-aminoquinolines,[26] 4-aminopyridine,[27] and 2-aminobenzimidazole.[28] We feel that the monocation **2** is formed by the same way as discussed in case of *o*-APBT or *m*-APBT and then undergoes a structural reorganization as shown in Scheme 3, leading to the species **2′**. In aqueous medium, the species **2** being highly solvated, this reorganization may be difficult and hence the species **2′** will have less contribution in the ground state. But in cyclohexane, the solvation is less and thus the species **2′** will be more favorable which is exhibited by the higher intensity of the longest wavelength band in

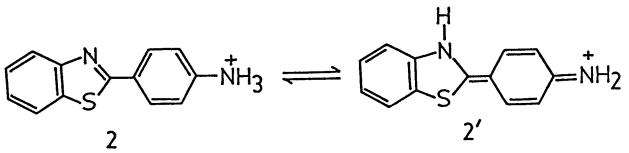

Scheme 3.

the monocation spectrum. As the $[H^+]$ is increased, the equilibrium is shifted towards the left and the second protonation occurs at the heterocyclic nitrogen atom giving rise to dication **3**. The resemblance between the absorption spectrum of *p*-APBT at H_o—4.0 and the absorption spectrum of the monocation of 2-PBT supports our explanation.

The fluorescence spectra, recorded for solutions in the pH range (in which the ground state equilibrium exists) by exciting at both the isosbestic points, show a gradual decrease in intensity of the 420 nm band and simultaneous appearance of 390 nm band as shoulder (only noticeable at pH 2.0) with the increase of $[H^+]$ until pH 0.5. The band width at half maximum also increases with increase of acid concentration. When the solutions having pH<3.0 were excited at 400 nm (where the neutral molecule does not absorb) a weak fluorescence band appears at ca. 445 nm, the intensity of which increases with the decrease of pH. The fluorescence excitation spectra at pH 1.5, recorded by monitoring the fluorescence maximum at 390 and 460 nm are different from each other. The former consists of a single band matching with the monocation absorption spectrum of *o*-APBT or *m*-APBT and the latter one consists of two bands at 390 and 340 nm matching with the absorption spectrum of the monocation. The ca. 300 nm absorption band may thus be due to a mixture of species **2** and **2′**. The full width at half maximum observed for the absorption and fluorescence excitation spectra are different form each other and thus supports our conclusion. Analogous to *o*-APBT and *m*-APBT the fluorescence band at 390 nm can be assigned to the fluorescence from monocation **2** having low fluorescence quantum yield. Thus the 445 nm band may be due to the species **2′**. The increase of fluorescence intensity of the 445 nm with further increase of $[H^+]$ can be attributed to the formation of dication **3**. This is because the fluorescence band maxima of the dications of other amines and the monocation of 2-PBT are also nearly at the same wavelength and are formed at the same acid concentration. This suggests that structural reorganization of species **2′** takes place before the dication **3** is formed and thus leading to same emission band maxima. The similar behavior has also been observed in 2-aminobenzimidazole[28] and 2- and 4-aminoquinolines.[26,27]

Table 5. Ground and Excited State pK_a Values for the Various Prototropic Reactions of *o*-APBT, *m*-APBT, *p*-APBT, and 2-PBT

Equilibrium	pK_a	pK_a^{*} [a]		
		Abs	Flu	Ft
o-APBT				
Dication⇄Monocation	−1.8	−0.2	2.0	
Monocation⇄Neutral	2.6	−6.9	−4.6	
Neutral⇄Monoanion	>16	—	—	
m-APBT				
Dication⇄Monocation	0.07	4.5	4.8	0.5
Monocation⇄Neutral	3.4	−3.4	−8.9	
Neutral⇄Monoanion	>16	—	—	12.4
p-APBT				
Dication⇄Monocation	0.1	—	—	
Monocation⇄Neutral	3.0	—	—	
Neutral⇄Monoanion	>16	—	—	
2-PBT				
Monocation⇄Neutral	0.7			1.0

Abs: Calculated from absorption spectra, Flu: Calculated from fluorescence spectra, Ft: Fluorimetric titration.

4. Acidity Constants. The pK_a values for different prototropic equilibria (Scheme 4) of the molecules have been determined using absorption data and are collected in Table 5. Since *p*-APBT is resonance stabilized (Scheme 1), the electron density at the amino nitrogen will be low which is reflected by the low pK_a value (3.0) for the monocation–neutral equilibrium compared to that (3.4) of *m*-APBT. The very low pK_a value for the monocation–neutral equilibrium in *o*-APBT than those of other molecules is due to the IHB formation. The pK_a value for the monocation–neutral equilibrium in 2-PBT is greater than the pK_a values for the corresponding dication–monocation equilibria of the amino derivatives. This is due to the presence of the $-\overset{+}{N}H_3$ group in their monocations, which withdraws electron density from the heterocyclic ring. Since, the $-\overset{+}{N}H_3$ group is more closer to the $\geqslant$N atom in *o*-APBT, the decrease of electron density on $\geqslant$N is more compared to other molecules. As a result, the pK_a for the dication-monocation equilibrium is less than that of *m*-APBT which is again lower than that of *p*-APBT.

The pK_a* values for the corresponding equilibria of the molecules including 2-PBT have also been determined by fluorimetric titrations and by Forster cycle calculations, wherever applicable. The results thus obtained are consistent with our conclusions that $-NH_2$ group becomes less basic and pyridinic nitrogen ($\geqslant$N) more basic on excitation to the S_1 state. Consequently,

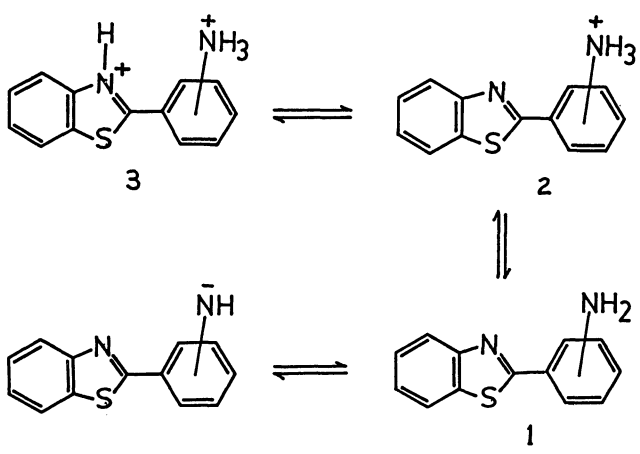

Scheme 4.

Table 6. Calculated Transition Energies (λ), Oscillator Strengths (f), Transitions Polarizations (α°) and Charge Densities at the Basic Centers of *o*-APBT, *m*-APBT, and *p*-APBT

Molecules	Transition energy(λ) (nm)	Oscillator strength (f)	Polarization (α°)[a]	π-Electron Density					
				Ground state			Excited state		
				S_1	N_3	N_{16}	S_1	N_3	N_{16}
1	2	3	4	5	6	7	8	9	10
	335	0.9286	359	1.5132	1.4332	1.9247	1.583	1.434	1.9
o-APBT(I)	303.8	0.3065	244						
	282	0.093	127						
	245.8	0.1277	98						
	346.5	0.9523	353	1.4846	1.680	1.919	1.501	1.728	1.8
o-APBT(IA)	298.0	0.189	284						
	290	0.1458	115						
	240	0.4855	312						
	327	0.9877	349	1.515	1.419	1.934	1.593	1.408	1.9
m-APBT	306	0.2855	233						
	284.9	0.1113	279						
	246	0.0682	100						
	333	1.1795	352	1.519	1.4229	1.9334	1.583	1.430	1.922
p-APBT	304	0.235	243						
	267	0.330	79						
	249	0.103	63.8						

a) α° is the angle made by the total transition moment vector with the positive direction of the long axis (directed towards the phenyl ring) of the molecule, measured anti-clockwise.

the pK_a*(1.0) is greater than pK_a(0.7) for 2-PBT. In other molecules fluorimetric titrations have resulted more or less the ground state pK_a values for the monocation–neutral equilibrium. This may be either due to the nonestablishment of the prototropic equilibrium in the S_1 state or no change occurring in pK_a value upon excitation. At present we are unable to specify which one of these mechanisms is playing the role.

The pK_a* values calculated by using the absorption band maxima and fluorescence band maxima are large and differ much from each other. This can be attributed to the difference in solvent relaxation of the conjugate acid-base pair in the S_0 and S_1 states and are consistent with the solvent relaxation data as discussed earlier. The Forster cycle method can not be used for *p*-APBT because of the failure of the assumptions made in the method.

5. Molecular Orbital Calculations. The molecular orbital calculations have been carried out for the three molecules and the hydrogen-bonded conformer of *o*-APBT by using Pariser, Parr, and Popple (PPP) method.[29–31] The parameters used for the calculations are taken from the paper by Dorr et al.[32] Other details of calculations are discussed in our earlier paper.[4]

Table 6 gives a list of values of transition energies (λ_{nm}) and the corresponding oscillator strength (f) and polarizations (α°) alongwith the π-electron densities at various basic centers. The experimental spectral data (Table 1) of *o*-APBT match more closely with those of calculated ones for its hydrogen-bonded conformation (IA). For other molecules also, the agreement between the calculated and the observed values is very good. As it is difficult to find 'f' experimentally, we are unable to compare the same with the calculated values. However, the f values for the corresponding transitions of the molecules are qualitatively consistent with the intensity ($\log\varepsilon$) of the absorption bands. As mentioned earlier, the transition moment corresponding to the longest wavelength band of the molecules is polarized towards the phenyl ring.

The data of Table 6 indicate that the π-electron density on the amino-nitrogen (N_{16}) is greater than that at the nitrogen atom (N_3) of the heterocyclic ring in both the S_0 and S_1 states. Thus, the first protonation should take place at the amino group. In the S_1 state, the electron density on N_{16} has decreased, but on N_3 it has increased, which predicts that the amino group becomes more acidic and the pyridinic nitrogen becomes more basic on excitation and are consistent with the pK_a* values of monocation–neutral and dication–monocation equilibria (Table 5). This change of charge density on the nitrogen atoms of *o*-APBT favors the formation of IHB leading to the structure IA (Scheme 2). Moreover, the calculated electron densities on the amino-nitrogen foretells that the pK_a values for monocation–neutral equilibria of the molecules will be in the order *o*-APBT (IA)<*p*-APBT<*m*-APBT and exactly the same thing can be found from Table 5.

Conclusions

The following conclusions can be made from the above study.

(i) Ultraviolet and fluorescence spectra as well as the

low pK_a value of monocation–neutral equilibrium confirm the presence of intramolecular hydrogen bonding in *o*-APBT in the S_0 and S_1 states.

(ii) Solvatochromic effects confirm that *m*-APBT is more polar in the S_1 state than *o*-APBT and *p*-APBT. Large Stokes shifts observed in protic solvents are due to the solute-solvent complex formation and the charge transfer structure of the S_1 state.

(iii) Molecular orbital calculations (PPP) as well as the pK_a values indicate that the first protonation occurs at the amino group in all the molecules. But in case of *p*-APBT, the structural reorganization of the monocation leads to the quinonoid structure. The similar study carried out in cyclohexane and trifluoroacetic acid indicates that the quinonoid form is more stable in the nonpolar solvents. The absorption, fluorescence, and excitation fluorescence spectra (recorded at 390 and 460 nm) indicate that the species **2** and **2′** are present simultaneous in both S_0 and S_1 states. The dication is formed by protonating amino as well as the tertiary nitrogen atom, having similar structure in each case.

(iv) Although the amino group becomes stronger acid and tertiary nitrogen atom more basic upon excitation, the prototropic equilibria are not established in S_1 state.

(v) Very small fluorescence quantum yield observed for normal Stokes-shifted fluorescence in nonpolar solvents indicates that the phototautomer formed in *o*-APBT is nonfluorescent. The increase of fluorescence quantum yield with hydrogen bonding solvents proves this.

The authors are thankful to the Department of Science and Technology, New Delhi for financial support to the project entitled "Proton transfer reactions in the excited states in micellar media".

References

1) a) E. Belgoderr, R. Bossio, S. Chimichi, V. Parrini, and R. Pepino, *Dyes Pigm.*, **4**, 59 (1983). b) Kalle & Co., A. G., Br. Patent 895001, April 26, 1962.

2) P. F. Barbara, L. E. Brus, and P. M. Rentzepis, *J. Am. Chem. Soc.*, **102**, 5631 (1980); D. L. Williams and A. Heller, *J. Phys. Chem.*, **74**, 4473 (1970); R. G. Brown, J. D. Hepworth, K. W. Hodgson, B. May, and M. A. West, *Chem. Ind. (London)*, **1982**, 129; R. S. Becker, C. Lenolele, and A. Zein, *J. Phys. Chem.*, **91**, 3509 (1987); R. S. Becker, C. Lenolele, and A. Zein, *J. Phys. Chem.*, **91**, 351 (1987); C. A. S. Potter and R. G. Brown, *Chem. Phys. Lett.*, **153** (**1**), 7 (1988) ; W. E. Brewer, M. L. Martinez, and P. T. Chou, *J. Phys. Chem.*, **94**, 1915 (1990).

3) a) P. C. Tway and L. J. Clinelove, *J. Phys. Chem.*, **86**, 5223, 5227 (1982); A. K. Mishra and S. K. Dogra, *Indian J. Phys., Sect. B,* **58**, 480 (1984); A. K. Mishra and S. K. Dogra, *Bull. Chem. Soc. Jpn.*, **58**, 3587 (1985). b) A. K. Mishra and S. K. Dogra, *J. Photochem.*, **31**, 333 (1985).

4) J. K. Dey and S. K. Dogra, *Chem. Phys.*, **143**, 97 (1990).

5) D. W. Hein, R. J. Alheim, and J. J. Leavitt, *J. Am. Chem. Soc.*, **79**, 427 (1957).

6) J. A. Riddick and W. B. Bunger, "Organic Solvents," Wiley Interscience, New York (1970), pp. 592—594, 798—805.

7) a) M. J. Jorgenson and R. D. Harter, *J. Am. Chem. Soc.*, **85**, 878 (1983). b) G. Yagil, *J. Phys. Chem.*, **71**, 1034 (1967). c) W. H. Melhuish, *J. Phys. Chem.*, **65**, 229 (1961).

8) M. Swaminathan and S. K. Dogra, *Indian J. Chem., Sect. A,* **22**, 853 (1983).

9) QCPE Program No. QCMP 007, Indiana University, Chemistry Department, U.S.A.

10) R. Passarini, *J. Chem. Soc.*, **1954**, 2256.

11) J. K. Dey and S. K. Dogra, *Indian J. Chem., Sect. A,* **29**, 1153 (1990).

12) J. N. Murrell, *Proc. Phys. Soc. London, Sect. A,* **68**, 969 (1955); H. C. Longuet-Higgins and J. N. Murrell, *Proc. Phys. Soc. London, Sect. A,* **68**, 601 (1955); M. Godfrey and J. N. Murrell, *Proc. R. Soc. London, Ser. A,* **278**, 57, 64, 71 (1964).

13) S .P. McGlynn, L. Vanquickenborne, M. Kinoshita, and D. G. Carroll, "Introduction to Applied Quantum Chemistry," ed by Holt, Rinehart, and Winston, New York, N.Y.; E. C. Lim and S. K. Chakrabarti, *J. Chem. Phys.*, **47**, 4726 (1964).

14) M. Kasha, "Light and Life," ed by W. D. McEtroy and B. Glass, John Hopkins University Press, Baltimore, Md. (1961), pp. 31—34; K. Kamura, H. Tsubomura, and S. Nagakura, *Bull. Chem. Soc. Jpn.*, **37**, 1336 (1964); K. Kamura and H. Tsubomura, *Mol. Phys.*, **11**, 349 (1966); J. C. D. Brand, D. R. Williams, and T. J. Cook, *J. Mol. Spectrosc.*, **20**, 359 (1966).

15) J. R. Merrill and R. Bennett, *J. Chem. Phys.*, **43**, 1410 (1965); J. A. Otterstedt, *J. Chem. Phys.*, **58**, 5716 (1973); H. Shizuka, K. Matsui, T. Okamura, and I. Tanaka, *J. Phys. Chem.*, **79**, 2731 (1975); W. F. Richy and R. S. Becker, *J. Phys. Chem.*, **49** (**3**), 2092 (1968); M. D. Cohen, G. M. J. Schmidt, and (in part) (Mrs.) S. Flavian, *J. Chem. Soc.*, **1964**, 2041; M. D. Cohen and (Mrs.) S. Flavian, *J. Chem. Soc. B,* **1967**, 317.

16) a) M. Swaminathan and S. K. Dogra, *J. Am. Chem. Soc.*, **105**, 6223 (1983). b) A. K. Mishra and S. K. Dogra, *Indian J. Chem., Sect. A,* **24**, 285 (1984). c) P. Phaniraj, A. K. Mishra, and S. K. Dogra, *Indian J. Chem., Sect. A,* **24**, 913 (1984).

17) S. G. Schulman and A. C. Capomacchia, *Anal. Chim. Acta,* **58**, 91 (1972).

18) E. C. Lim and Jack M. H. Yu, *J. Chem. Phys.*, **45**, 4712 (1966); H. Shizuka, M. Eukushima, T. Fuju, T. Kobayashi, H. Ohtani, and M. Hoshino, *Bull. Chem. Soc. Jpn.*, **58**, 2107 (1985).

19) E. Lippert, *Z. Naturforsch., A,* **10**, 541 (1955).

20) E. M. Kosower, *J. Am. Chem. Soc.*, **80**, 3253 (1958).

21) K. Dimroth, C. Reichardt, T. Siepmann, and F. Bohlmann, *Liebigs Ann. Chem.*, **661**, 1 (1983); C. Reichardt, *Angew. Chem.*, **91**, 119 (1979).

22) S. Majumdar, R. Manoharan, and S. K. Dogra, *J. Photochem. Photobiol., A: Chem.*, **46**, 301 (1989).

23) L. Coosemans, F. C. DeSchryver, and A. Van Dormael, *Chem. Phys. Lett.*, **65**, 95 (1979).

24) R. O. Loutfy and A. C. Somersall, *Can. J. Chem.*, **54**, 760 (1976); G. E. Johnson, *J. Phys. Chem.*, **84**, 2940 (1980); T. Takahashi, K. Kikuchi, and H. Kokuban, *J. Photochem.*, **14**, 67 (1980).

25) Th. Forster, *Z. Elektrochem.*, **54**, 42 (1950).

26) P. J. Kovi, A. C. Capomacchia, and S. G. Schulman,

Anal. Chem., **44**, 1611 (1972).
27) A. Albert, R. J. Goldacre, and J. Phillips, *J. Chem. Soc.*, **1948**, 2240; *J. Chem. Soc.*, **1943**, 454; *J. Chem. Soc.*, **1946**, 706; H. C. Longuet-Higgins, *J. Chem. Phys.*, **18**, 275 (1951).
28) A. K. Mishra and S. K. Dogra, *Indian J. Chem., Sect. A*, **24**, 815 (1985).
29) R. Pariser and R. G. Parr, *J. Chem. Phys.*, **21**, 466, 767 (1953).
30) J. A. Pople, *Trans. Faraday Soc.*, **49**, 1315 (1953).
31) J. Delbene and H. H. Jaffe, *J. Chem. Phys.*, **48**, 1807 (1968).
32) Von F. Dorr, G. Hohlneicher, and S. Schneider, *Ber. Bunsen-Ges. Phys. Chem.*, **70**, 803 (1966).